Eurasian Journal of Physics and Functional Materials

Volume 8 | Number 1

Article 4

Pages: 33 - 44

3-22-2024

Luminescence and creation of electron-hole trapping centers in alkali metal sulfates activated by Pb2+ impurity

T. N. Nurakhmetov
L.N. Gumilyov Eurasian National University, Astana, Kazakhstan

R. K. Shamieva
L.N. Gumilyov Eurasian National University, Astana, Kazakhstan, rasha_arman@bk.ru

Zh. M. Salikhodzha
L.N. Gumilyov Eurasian National University, Astana, Kazakhstan

N. I. Temirkulova
L.N. Gumilyov Eurasian National University, Astana, Kazakhstan

T. T. Alibay
L.N. Gumilyov Eurasian National University, Astana, Kazakhstan

See next page for additional authors

Recommended Citation

Nurakhmetov, T. N.; Shamieva, R. K.; Salikhodzha, Zh. M.; Temirkulova, N. I.; Alibay, T. T.; Sadykova, B. M.; Yussupbekova, B. N.; and Kabdulkak, A. A. (2024) "Luminescence and creation of electron-hole trapping centers in alkali metal sulfates activated by Pb2+ impurity," *Eurasian Journal of Physics and Functional Materials*: Vol. 8: No. 1, Article 4.
DOI: https://doi.org/10.32523/ejpfm.2024080104

Luminescence and creation of electron-hole trapping centers in alkali metal sulfates activated by Pb2+ impurity

Authors

T. N. Nurakhmetov, R. K. Shamieva, Zh. M. Salikhodzha, N. I. Temirkulova, T. T. Alibay, B. M. Sadykova, B. N. Yussupbekova, and A. A. Kabdulkak

Eurasian Journal of Physics and Functional Materials

2024, 8(1), 33-44

Luminescence and creation of electron-hole trapping centers in alkali metal sulfates activated by Pb^{2+} impurity

T.N. Nurakhmetov, R.K. Shamieva*, Zh.M. Salikhodzha, N.I. Temirkulova, T.T. Alibay, B.M. Sadykova, B.N. Yussupbekova, A.A. Kabdulkak

L.N. Gumilyov Eurasian National University, Astana, Kazakhstan

E-mail: rasha_arman@bk.ru

DOI: **10.32523/ejpfm.2024080104**
Received: 20.01.2024 - after revision

The nature of the impurity emission and the process of creating intrinsic and impurity electron-hole trapping centers were studied by spectroscopic and thermal activation methods in Na_2SO_4 - Pb and K_2SO_4 - Pb phosphors. The combined radiative electronic state is formed from intrinsic SO_4^{3-} - SO_4^- and impurity Pb^+ - SO_4^- electron-hole trapping centers in UV-irradiated phosphors with a photon energy of 6.2 eV at 80 K. Emissions of 3.2 eV and 3.6 eV resulting from irradiation with photons with an energy of 6.2 eV are associated with intracenter transitions of $3p_1$ - $1s_0$ in Pb^{2+} located in nonequivalent positions of the Na_2SO_4 lattice.

Keywords: electron; hole; recombination emission; intrinsic emission; sulfate; excitation

Introduction

Phosphors doped with Pb^{2+} can be used in X-ray imaging devices, low-pressure lamps, and high-energy physics [1]. Crystalline $PbSO_4$ is applied as a scintillator for high-energy gamma radiation. The decay time ranges from 10 ns to 150 ns. The emission spectrum is at 3.14 eV and drops by 10% of the maximum intensity in the range of 5.17 eV to 2.8 eV at 300 K [2, 3].

In a matrix of sulfates of alkaline earth metals $CaSO_4$, $BaSO_4$ and $SrSO_4$ with impurities of Pb^{2+}, *Folkerts et al.* [4] discovered luminescence with a small Stokes shift. In these matrices, electrons transfer from the $1s_0$ ground state to the $3p_{0,1,2}$ triplet state and the $1p_1$ singlet state of the Pb^{2+} impurity. At low temperatures, the excitation in the triplet state relaxes to the lowest excited metastable state $3p_0$. According to the authors of [4], the forbidden transition $3p_0$ - $1s_0$ is responsible for the emission that appears at low temperatures and has a long decay time. At higher temperatures, the $3p_1$ level begins to fill, and the decay time becomes significantly shorter since the emission arising during the $3p_1$ - $1s_0$ transition is allowed due to spinorbital interactions [4]. In $CaSO_4$ - Pb^{2+}, upon excitation in the vacuum-ultraviolet region, absorption bands at 7.7 eV, which are attributed to the $1s_0$ - $1p_1$ electron transition, were observed [4]. In phosphates and borates, the fundamental absorption of the matrix begins at approximately 7.7 eV. The authors suggest that the band at 7.7 eV is too wide to absorb only the C-band $1s_0$ - $1p_0$ of the Pb^{2+} impurity. Most likely, D-band absorption and lattice absorption also contribute to the sulfate matrix [4].

In the works of the authors [5], $Ca_3(BO_3)_2$ - Pb^{2+} emission bands with a minimal Stokes shift were detected at 3.4 eV and 3.7 eV when excited by photons at 4.6 eV. Other authors have estimated the optimal concentration of Pb^{2+} impurities at which intense emission occurs. Emissions occur during the transition of electrons from $3p_1$ - $1s_0$ to Pb^{2+} impurities in the matrix [6–11].

Pb^{2+} impurities introduced into the $LiEuMo_2O_8$ phosphor act as sensitizers that transfer energy from the matrix to the Eu^{3+} emitters [12].

The authors' work [12, 13] showed that in $Ca_{10-x}Pb_x(PO_4)_6(OH)_2Y$ compounds, two broad emission bands, corresponding to two transitions $3p_1$ - $1s_0$, appear when excited by lasers with an energy of 4.6 eV at room temperature. The blue band at 2.8–3.1 eV is excited at a photon energy of 3.5 eV, and the short-wavelength band at 3.65–3.8 eV, corresponding to the $3p_1$ - $1s_0$ transition, is excited at a photon energy of 5.1 eV. Substituted Ca^{2+} ions in the Ca I and Ca II positions: blue emission at 2.8 eV arises from Pb^{2+} in the Ca II position, and ultraviolet emission at 3.65 eV arises from Pb^{2+} in the Ca I position. At a low temperature of 25 K, the broad band shifts to the shortwavelength region of the spectrum. The authors of [13] did not exclude the possibility that mixing of the $3p_1$ and $3p_0$ levels at low temperatures can be achieved by the $3p_0 \rightarrow 1s_0$ transition of Pb^{2+} positions in the Ca II matrix upon excitation with a photon energy of 3.5 eV.

Weak shortwavelength emission is detected at 4.2 eV, which is excited by photons at 5.7 eV, 5.0 eV and 4.7 eV in $BaAl_2O_4$ - Pb^{2+} [14]. These emission bands are attributed to the $3p_1 \rightarrow 1s_0$ transition at two Pb^{2+} positions in the lattice, which substitutes Ba^{2+} ions at temperatures of 4 K and 80 K. The longwavelength emission band at 2.8–3.1 eV is associated with a charge transfer transition involving Pb^{2+} ions near the exciton state (D state). During the process of charge transfer from the excited anion to the impurities, electron-hole trapping centers should be formed.

In this work, the nature of the impurity emission Pb^{2+} and the formation of electron-hole trapping centers as a result of charge transfer from the matrix to

impurities Na_2SO_4 - Pb , $PbSO_4$ and K_2SO_4 - Pb are investigated.

Experimental

Highly pure sodium and potassium sulfates (99.99% purity, Sigma Aldrich) and lead (II) sulfate powders (Sigma Aldrich) were used as the raw materials. Na_2SO_4 - Pb samples were obtained by the slow evaporation method. The volume of Na_2SO_4 powder was determined according to the stoichiometric ratio. A precalculated amount of $PbSO_4$ impurity was added to Na_2SO_4 and mixed.Concentrated sulfuric acid was used to dissolve the mixed powder. After complete dissolution, the solution was washed several times with double distilled water and dried at 70° C. After this, the sample was sintered at 400° C for 5 hours in an argon atmosphere. Cooling of the annealed powder was carried out slowly over several hours. The finished samples were turned into tablet form at 0.05 MPa. A crystal of potassium sulfate with Pb impurity was obtained by evaporation method from a saturated aqueous solution in temperature of 40° C.

Chemical analysis (EDX) was carried out on a TESCAN VEGA 3 LMH scanning electron microscope with a microanalyzer system from Oxford Instruments (UK). The resolution was 3 nm at 30 kV (SE), 6 nm at 30 kV (BSE), the magnification was 6X-300000X, and the screening magnification was 12X-600000X.

The samples were studied by spectroscopic and thermal activation methods. Emission and excitation spectra were measured with a CM 2203 spectrofluorimeter (Republic of Belarus) in the spectral range of 1.5–6.2 eV (at room temperature). The measurement error was 0.01 nm. A low-temperature study was performed on a cryostat cooled with liquid nitrogen (77 K).

X-ray luminescence was carried out on a BSV-23 installation using an X-ray tube with a copper anode. The operating mode of the BSV-23 was a current of 10 mA and a voltage of 40 kV, and the photon energy was 10–15 keV.

XRD analysis was performed on DRON-7 diffractometer. Independent rotation around the 2θ and θ axes allows the device to be used for solving a number of single-crystal diffractometry problems. DRON-7 has a Cu anode.

Results

The chemical compositions of the obtained samples were studied using a scanning electron microscope (SEM) and energy dispersive analysis. SEM-EDX images of the Na_2SO_4 - Pb results are shown in Figure 1. The obtained results correspond to theoretical calculations of the percentage of element components. From the SEM results, it can be seen that the sample is composed of particles having different sizes of approximately 5–200 μm (Figure 1a). According to the SEM-EDX results, a large number of peaks were recorded (Figure 1b), characteristic of metal ions, such as Na-16.9%, S-11.6%, O-67.3% and Pb-3.9%, which confirmed the presence of Pb impurities and its percentage in the Na_2SO_4 powder. The EDX pictures of K_2SO_4 - Pb and the percentage (1d) of elements in K_2SO_4 - Pb

(K-33.13%, S-15.57%, O-31.65%, Pb-5.43%) are shown in Figure 1c.The presence of Pb impurity in K_2SO_4 - Pb is confirmed by SEM-EDX (Figure 1d).

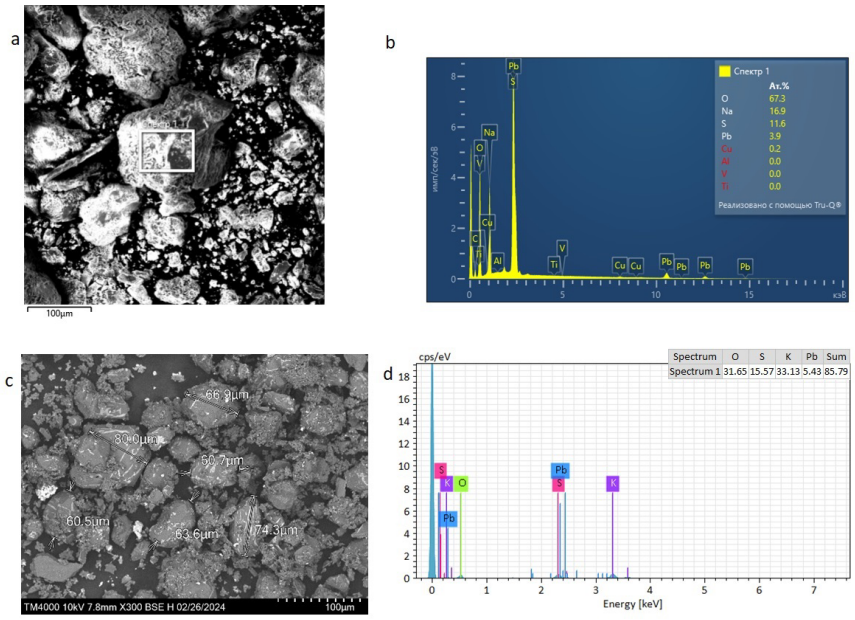

Figure 1. SEM-EDX image of Na_2SO_4 - Pb and K_2SO_4 - Pb.

An analysis of a specific area was also carried out, which shows the distribution of each of the elements Na_2SO_4 - Pb shown in Figure 2.

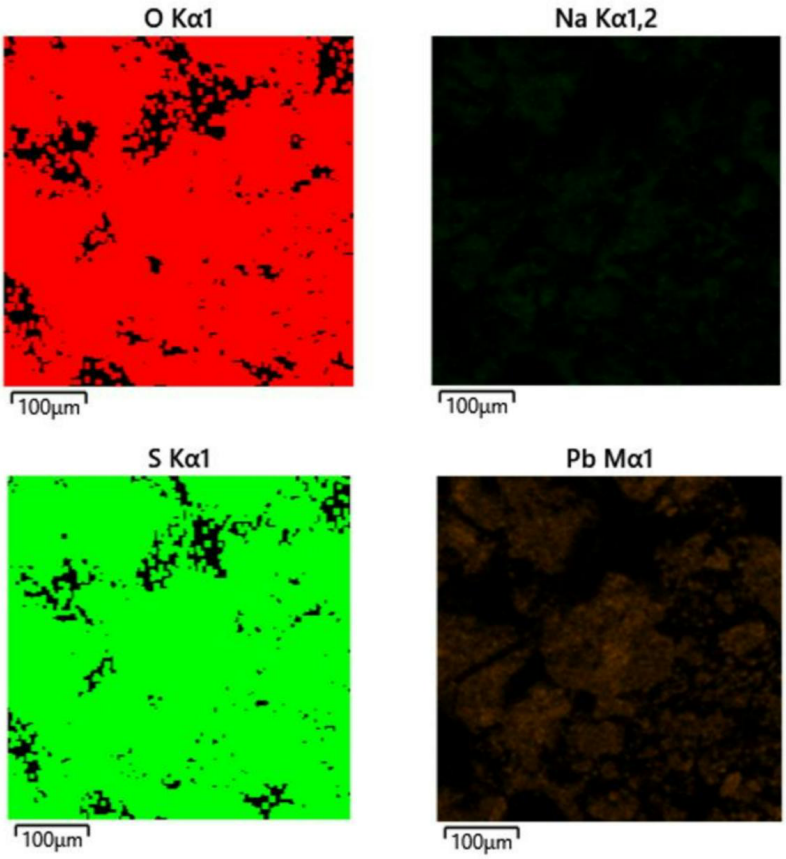

Figure 2. Distribution map of chemical elements in Na_2SO_4 - Pb powder.

Using X-ray diffraction, a cubic structure similar to the structure of "Entry-96-591-0102" with space group Pm-3m (211) was confirmed.

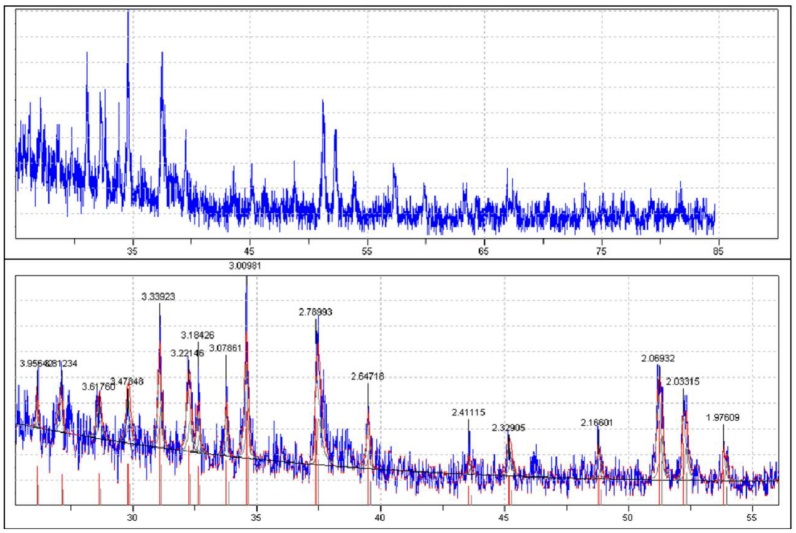

Figure 3. X-ray diffraction pattern of Na_2SO_4 - Pb powder.

In transition metal oxides excited by ultraviolet photons and activated by Pb^{2+} ions at different temperatures, emissions arise at 4.2 eV, 3.2–3.6 eV and 2.9–3.1 eV at corresponding excitation energies as mentioned above.

The emission spectrum of $PbSO_4$ when excited by photons with an energy of 6.2 eV is shown in Figure 4. It can be seen that emissions appear at 3.65 eV, 3.3–3.4 eV and 2.9–3.1 eV. Emissions at 3.65 eV and 2.9 eV (curve 1) are excited at photon energies of 6.0 eV and 5.5 eV (curves 2 and 3). Similar results were obtained by the authors of [1–3].

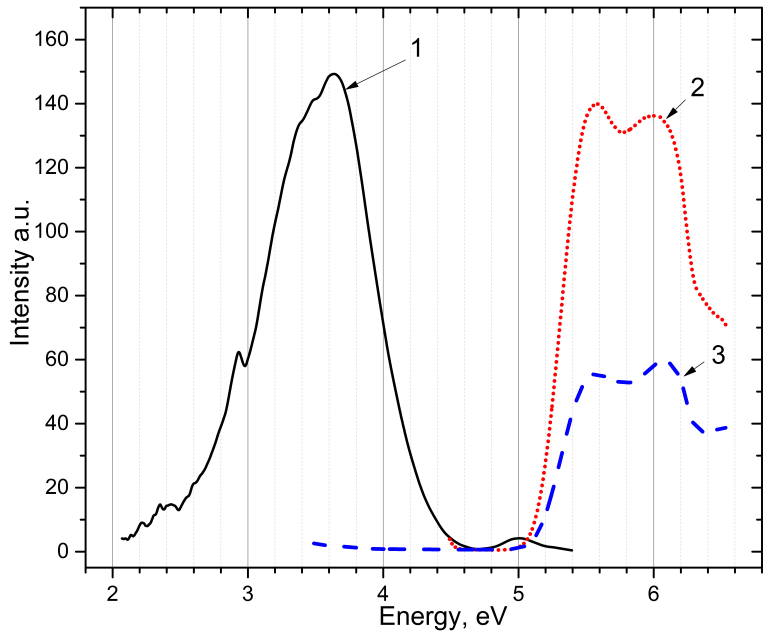

Figure 4. Emission and excitation spectrum of $PbSO_4$ at 297 K (curve 1 – emission spectrum excited by 6.2 eV; curve 2, 3 – excitation spectrum of emissions at 3.65 eV and 2.9 eV.

In the next stage, emission spectra of Na_2SO_4 - Pb were studied. The emission

spectra of Na_2SO_4 - Pb when excited by photons at 6.2 eV at 80 K (curve 1) and at 297 K (curve 2) are shown in Figure 5.

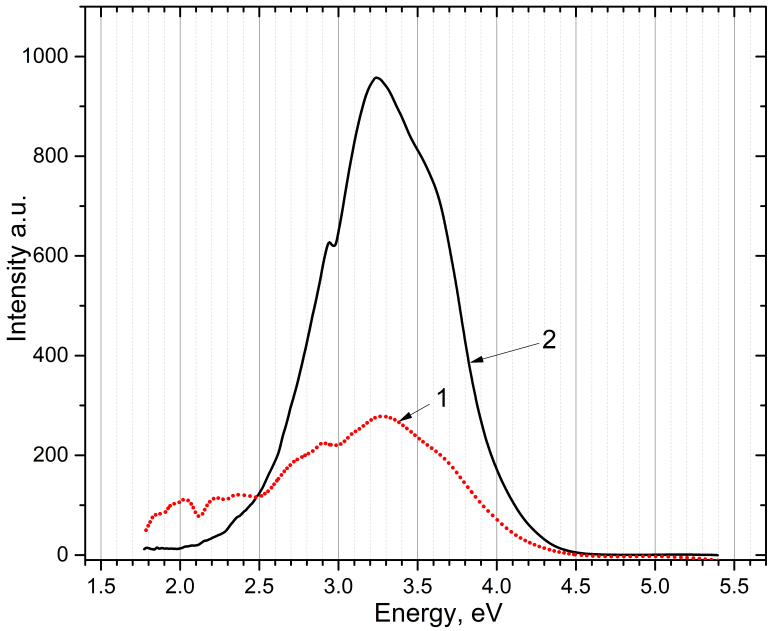

Figure 5. Emission spectra of Na_2SO_4 - Pb when excited by photons at 6.2 eV at 80 K (curve 1) and at 297 K (curve 2).

The emission bands appear at 3.65 eV, 3.2 eV, 2.9 eV and 2.7 eV at 297 K (curve 1) and 80 K (curve 2).

The excitation spectra of the 3.6 eV and 2.9 eV emission bands are shown in Figure 6. It can be seen form Figure 6 (curve 1) that the emission band at 3.6 eV is excited at photon energies of 5.7 eV and 6.0 eV at 80 K. The emission band at 2.9 eV is excited at photon energies of 4.6 eV and 3.9 eV (curve 3) in the matrix transparency region and in the fundamental region at 5.5 eV and 6.0 eV at 297 K. It is assumed that the excitation bands at 4.65 eV and 3.9 eV are associated with the formation of trapping centers in irradiated crystals.

To determine the nature of the recombination emission at 2.9 eV, which is excited in the transparent region of Na_2SO_4, the sample was preliminarily irradiated with an energy of 6.2 eV, which create trapping centers. Then, in Na_2SO_4 - Pb, with induced trapping centers, the emission spectra upon excitation by photons with energies of 4.65 eV and 3.9 eV were measured.

The spectrum of recombination emission at 2.9 eV irradiated by photons with energies of 4.65 eV (curve 1) and 4.0 eV (curve 2) at 80 K are shown in Figure 7. It can be seen that in the spectrum, emission again appears at 2.9 eV, which was created by UV irradiation with an energy of 6.2 eV. These experimental data indicate that these recombination emissions of 2.9 eV are associated with the radiative decay of the trapping center created by UV irradiation.

The temperature dependence of the intensity of the main emission bands upon excitation by photons with an energy of 6.2 eV is shown in Figure 8 for 3.5 eV (curve 1), 3.2 eV (curve 2) and 2.9 eV (curve 3) from 80 K to 450 K. The emission intensity of 2.9 eV gradually decreases in the temperature range of 120–180 K, 200–250 K and a temperature increase at 280–320 K, and the intensity decreases to 450 K. The emission intensity at 3.5 eV and 3.2 eV monotonically

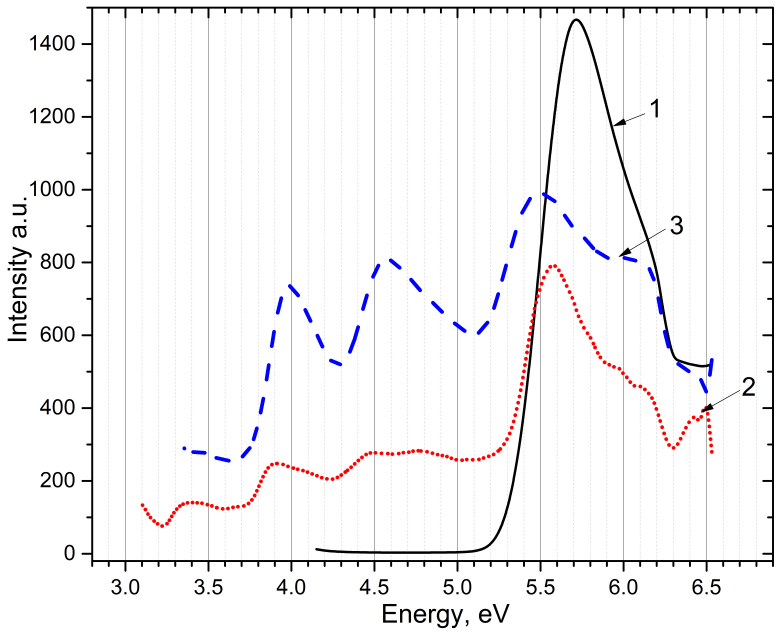

Figure 6. Excitation spectra of Na_2SO_4 - Pb emission bands: 3.6 eV at 80 K (curve 1); 2.9 eV at 80 K (curve 2); 2.9 eV at 297 K (curve 3).

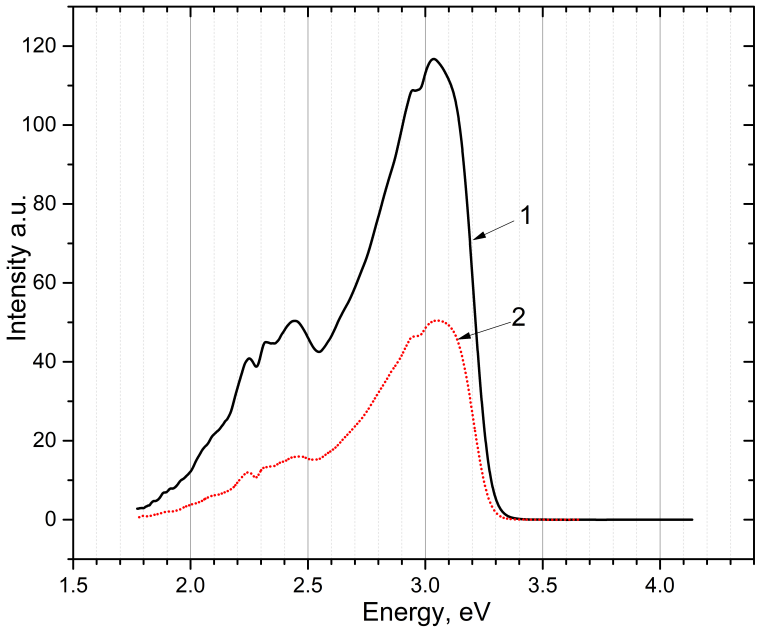

Figure 7. Emission spectra at 2.9 eV for Na_2SO_4 - Pb irradiated with photons with energies of 4.65 eV (curve 1) and 4.0 eV (curve 2) at 80 K.

decreases to 250 K and flares up at 250–320 K.

In the next step, the thermally stimulated luminescence (TSL) of the K_2SO_4 - Pb compound irradiated with X-rays at 80 K for 10 minutes was measured. The TSL spectra are shown in Figure 9. Figure 9 (a) clearly shows that at K_2SO_4 - Pb, when heated from 80 K to 450 K, TSL peaks appear at 160–180 K, 220–260 K, 300–360 K and 420–450 K. Figure 9 (b) shows the spectral composition of the main intense TSL peak at 300–360 K. In this TSL peak, a broad emission band appears at 4.1-4.2 eV. TSL peaks occur at those temperatures where the emission intensity decreases and increases at 2.9 eV, 3.2 eV and 3.5 eV as a function of temperature.

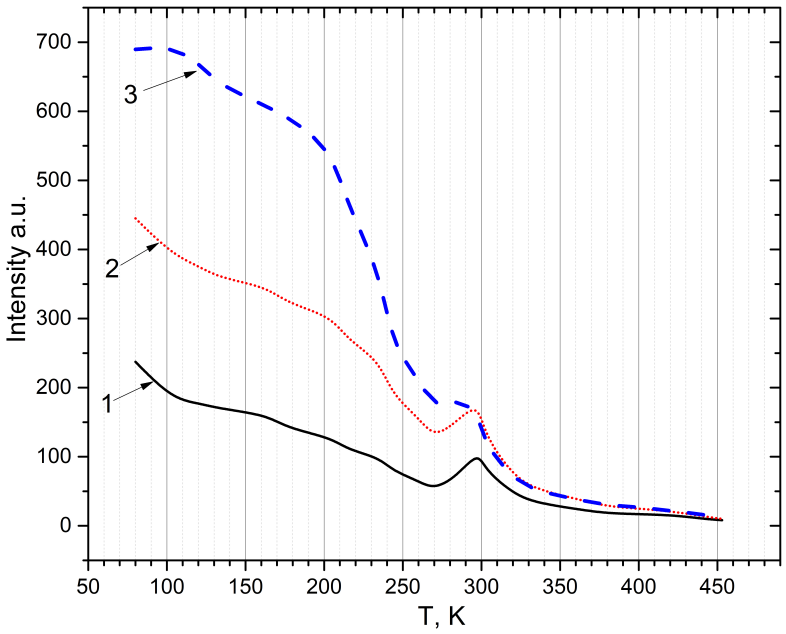

Figure 8. Temperature dependence of emission upon excitation by photons with an energy of 6.2 eV for Na_2SO_4 - Pb powder.

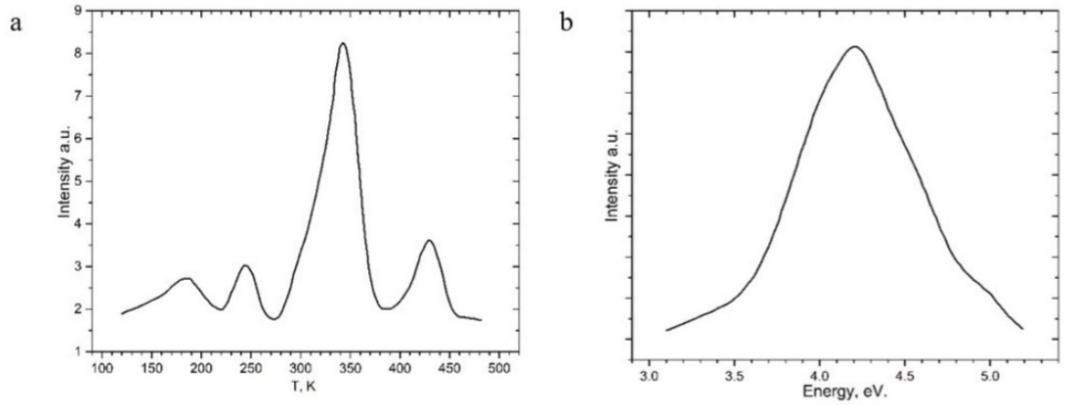

Figure 9. Thermally stimulated luminescence of K_2SO_4 - Pb irradiated with X-rays at 80 K for 10 minutes and the spectral composition of the main TSL peak.

The X-ray luminescence of K_2SO_4 - Pb is shown in Figure 10. It is clear that in K_2SO_4 - Pb , X-ray luminescence (curve 1) and phosphorescence (curve 2) appear in the spectral region of 4.1–4.2 eV. Besides, an additional X-ray luminescence peak appears in the region of 5.0–5.4 eV.

The temperature dependence of the main emissions arising from X-ray luminescence in K_2SO_4 - Pb is shown in Figure 11. It is obviously form Figure 11 (curve 1) that the emission at 4.1–4.2 eV, which occurs during X-ray excitation and phosphorescence, is exponentially quenched in the temperature range of 180–220 K, where the emission at 2.9 eV generally decreases to the maximum (Figure 8, curve 3).

The temperature dependence of the 5–5.4 eV emission that appears in the X-ray luminescence spectrum of K_2SO_4 - Pb appears in the form of increasing emission bands in those temperature ranges where TSL peaks appear. Emissions arising in the spectral range should be associated with the delocalization of electron-hole trapping centers. The recombination emission arising at these temperatures is

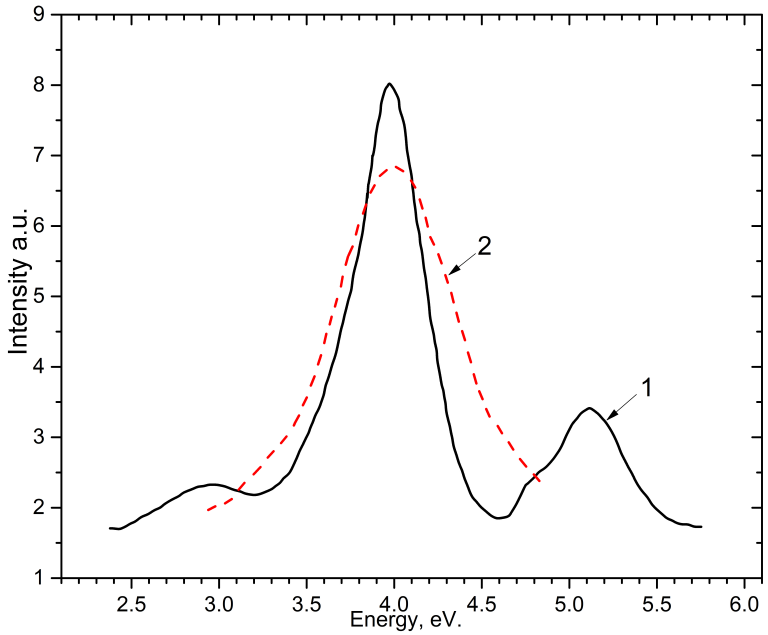

Figure 10. X-ray luminescence (curve 1) and phosphorescence (curve 2) at 80 K.

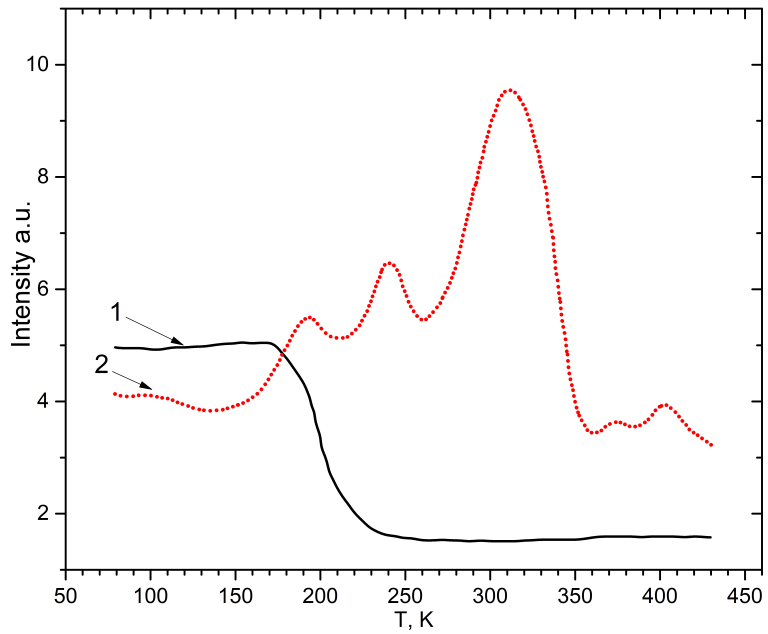

Figure 11. Temperature dependence of the main emissions arising from X-ray luminescence in K_2SO_4 - Pb.

transferred to Pb^{2+} impurities.

Discussion

In the works of the authors [4, 14], it was assumed that the emission bands at 4.2 eV, 3.6–3.7 eV and 3.2–3.4 eV are associated with the intracentre emission of the Pb^{2+} ion located in the matrix in nonequivalent positions when replacing main cations in the lattice. These emissions correspond to the transition of $3p_1$ excited electronic states to the $1s_0$ ground state of the Pb^{2+} impurity.

In the present study, emissions of the 3.5–3.6 eV and 3.2 eV bands appear.

It was assumed that these bands are associated with two states of Pb^{2+} in the matrix Na_2SO_4 and K_2SO_4. In the Na_2SO_4 and K_2SO_4 lattices, the K^+ and Na^+ ions occupy two nonequivalent positions. The impurity ion Pb^{2+}, when replacing the K^+ and Na^+ ions, can occupy two nonequivalent positions. The authors of [4, 14] associated the long-wavelength emission bands of 2.9–3.1 eV with a transition from the so-called c D state to the ground $1s_0$ state of the Pb^{2+} impurity. In some works [14], this band at 2.9–3.1 eV was associated with a transition from mixed $3p_1$ states by the metastable $3p_0$ state to the ground state $1s_0$. The authors of [14] suggested that the D state is connected by a combination of an exciton state with an impurity state resulting from charge transfer from the excited anion state to the impurities. Our experimental results in K_2SO_4 - Pb showed that, when X-ray luminescence and phosphorescence were measured at 80 K, recombination emission occurred at 4.1–4.2 eV and 5.0–5.4 eV. Phosphorescence or tunnel luminescence occurs at induced electron-hole trapping centers [15]. The nature of the X-ray luminescence should also be associated with recombination processes at trapping centers [16]. Measurements of the temperature dependences of the emission intensity of 4.1–4.2 eV showed that the emission is exponentially quenched in the temperature region at 180–230 K, where electron-hole trapping centers with emission decay by recombination occur [17].

Measurements of the temperature dependences of the main emission bands at 2.9–3.1 eV in K_2SO_4 - Pb demonstrate the presence of a TSL peak, and the flare-up of shortwavelength emission at 5.0–5.4 eV occurs in the same temperature regions. This is due to the decay of the induced electron-hole trapping centers that arise during UV and X-ray irradiation at 80 K.

Based on the experimental results, it is assumed that when irradiation occurs with photons with an energy of 6.2 eV, the created electrons are trapped by Pb^{2+} impurities, and according to the reaction $Pb^{2+} + e^- \rightarrow Pb^+$, electronic trapping centers are created complementary to the hole SO_4^-. Thus, in irradiated Na_2SO_4 and Na_2SO_4 - Pb, intrinsic trapping centers SO_4^{3-} - SO_4^- [18–22] and impurity trapping centers Pb^+ - SO_4^- are created. Radiative states consisting of trapping centers SO_4^{3-} - SO_4^- and Pb^+ - SO_4^- form combined radiative states below the conduction band at 3.1 eV and 2.9 eV [23, 24].

Combined radiative states are an analogue of the D-states of exciton radiative states near the impurity state Pb^{2+} in the conduction band, as suggested by the authors of [14].

Longwavelength emission at 2.9-3.1 eV in compounds $BaSO_4 : Pb^{2+}$, $SrSO_4 : Pb^{2+}$, AB_2O_4 ($A = Sr^{2+}, Ba^{2+}$; $B = Al^{3+}, Ga^{3+}$) and $AB_{12}O_{19}$ ($A = Sr^{2+}, Pb^{2+}$; $B = Al^{3+}, Ga^{3+}$) was attributed to the transition from the D-state to ground state $1s_0$ of the Pb^{2+} impurity by the authors of [4, 14]. Thus, we assume that longwavelength emissions of 2.9 eV and 3.1 eV are associated with the formation of a combined radiative state consisting of intrinsic and impurity electron-hole trapping centers in irradiated Na_2SO_4 - Pb and K_2SO_4 - Pb.

Conclusion

The emissions at 3.2 eV and 3.6 eV resulting from irradiation with photons with an energy of 6.2 eV are associated with the intracenter transition from $3p_1 \rightarrow 1s_0$ to Pb^{2+} located in nonequivalent positions in the Na_2SO_4 - Pb lattice.

Emissions arising from UV irradiation with photons of 6.2 eV at 2.9–3.1 eV are associated with the formation of a combined radiative electronic state consisting of intrinsic and impurity electron-hole trapping centers SO_4^{3-} - SO_4^- and Pb^+ - SO_4^- at 80 K.

References

[1] H.F. Folkerts, J. Zuidema, G. Blasse, Solid State Communications **99**(9) (1996) 655–658. [*CrossRef*]
[2] G. Blasse, Chemical Physics Letters **35**(3) (1975) 299–302 [*CrossRef*]
[3] W.W. Moses, S.E. Derenzo, P.J. Shlichta, IEEE Transactions on Nuclear Science **39**(5) (1992) 1190–1194. [*CrossRef*]
[4] H.F. Folkerts, M.A. Hamstra, G. Blasse, Chemical Physics Letters **246**(1-2) (1995) 135–138 [*CrossRef*]
[5] A.B. Gawande, R.P. Sonekar, S.K. Omanwar, International Journal of Optics **2014** (2014) 418459. [*CrossRef*]
[6] G. Blasse, B.C. Grabmaier, Luminescent Materials. Springer, Berlin, Heidelberg (1994) pp 1-9. [*CrossRef*]
[7] I. Pekgozlu, S. Tascialu, A. Menger, Inorganic Materials **44** (2008) 1151–1154.[*CrossRef*]
[8] A. Manavbasi, J.C. LaCombe, Journal of luminescence **128**(1) (2008) 129–134. [*CrossRef*]
[9] S.F. Wang et al., Inorganic Chemistry Communications **6**(2) (2003) 185–188. [*CrossRef*]
[10] Z. Xiu et al., Journal of Alloys and Compounds **441**(1-2) (2007) 219–221. [*CrossRef*]
[11] G. Blasse, Physics Letters A **28**(6) (1968) 444–445. [*CrossRef*]
[12] P. Dai, Ceramics International **43**(1) (2017) 1565–1570 [*CrossRef*]
[13] M. Mehnaoui et al., Optical Materials **30**(11) (2008) 1672–1676. [*CrossRef*]
[14] H.F. Folkerts, F. Ghianni, G. Blasse, Journal of Physics and Chemistry of Solids **57**(11) (1996) 1659–1665 [*CrossRef*]
[15] T.N. Nurakhmetov et al., Eurasian Journal of Physics and Functional Materials **5**(1) (2021) 24–30. [*CrossRef*]
[16] B.N. Yussupbekova et al., Nuclear Instruments and Methods in Physics Research Section B: Beam Interactions with Materials and Atoms **481** (2020) 19–23. [*CrossRef*]
[17] T.N. Nurakhmetov et al., Eurasian Journal of Physics and Functional Materials **5**(2) (2021) 140–147. [*CrossRef*]
[18] T.N. Nurakhmetov et al., Optik **242** (2021) 167081.[*CrossRef*]

[19] Zh.M. Salikhodzha et al., Radiation Measurements **125** (2019) 19–24. [*CrossRef*]
[20] T.N. Nurakhmetov et al., Optik **185** (2019) 156–160. [*CrossRef*]
[21] T.N. Nurakhmetov et al., Eurasian Journal of Physics and Functional Materials **3**(4) (2019) 330–338. [*CrossRef*]
[22] T. N. Nurakhmetov et al., Eurasian Journal of Physics and Functional Materials **5**(3) (2021) 200–208. [*CrossRef*]
[23] T.N. Nurakhmetov et al., Crystals **13**(7) (2023) 1054. [*CrossRef*]
[24] T.N. Nurakhmetov et al., Crystals **13**(11) (2023) 1596. [*CrossRef*]